σ-Donor Ligands | Hot Paper

Geometrically Constrained Cationic Low-Coordinate Tetrylenes: Highly Lewis Acidic σ-Donor Ligands in Catalytic Systems

Philip M. Keil and Terrance J. Hadlington*

Dedicated to Professor Matthias Driess on the occasion of his 60th birthday

Abstract: *A novel non-innocent ligand class, namely cationic single-centre ambiphiles, is reported in the phosphine-functionalised cationic tetrylene Ni^0 complexes, $[^{PhR}DippENi (PPh_3)_3]^+$ (**4a/b** (Ge) and **5** (Sn); $^{PhR}Dipp = \{[Ph_2PCH_2SiR_2](Dipp)N\}^-$; R = Ph, ^iPr; Dipp = $2,6-^iPr_2C_6H_3$). The inherent electronic nature of low-coordinate tetryliumylidenes, combined with the geometrically constrained [N–E–Ni] bending angle enforced by the chelating phosphine arm in these complexes, leads to strongly electrophilic E^{II} centres which readily bind nucleophiles, reversibly in the case of NH_3. Further, the Ge^{II} centre in **4a/b** readily abstracts the fluoride ion from $[SbF_6]^-$ to form the fluorogermylene complex $^{PhR}DippGe(F)Ni(PPh_3)_3$ **9**, despite this Ge^{II} centre simultaneously being a σ-donating ligand towards Ni^0. Alongside the observed catalytic ability of **4** and **5** in the hydrosilylation of alkynes and alkenes, this forms an exciting introduction to a multi-talented ligand class in cationic single-centre ambiphiles.*

Introduction

Singlet tetrylenes are by their nature single-centre ambiphiles, and can thus act as both σ-donor ligands and simultaneously accept electron density at the tetryl element centre.[1] Classical Fischer carbenes demonstrate this character through forming often reactive double-bonds with a transition metal,[2] due to the high π-acceptor character of the vacant *p*-orbital at carbon. On the contrary, electronically saturated N-heterocyclic carbenes, stabilized by considerable N→C donation, act as strong σ-donors but poor electron acceptors, and hence behave as innocent spectator ligands.[3] Heavier tetrylenes, due to an increased HOMO–LUMO separation, have a lessened propensity to partake in multiple bonding;[4] nevertheless a number of multiply bonded heavier group 14 element–transition metal complexes are now known,[1b,5] the seminal examples of which

were reported by the group of Power, and were accessed through the expedient salt metathesis of halo-tetrylenes with anionic metal fragments.[6] Similar complexes have been accessed recently by the same group through the metathesis of E–E and Mo–Mo triple bonds (E = Ge, Sn, Pb), akin to alkyne metathesis.[7] In search for a ligand class which can behave both as a Lewis base (i.e. a σ-donor) and a Lewis acid (i.e. an electron acceptor), we sought to further amplify the Lewis acidity of heavier tetrylene ligands through generating tetryliumylidene species, which are cationic and hence have a second vacant *p*-orbital when compared with their neutral counterparts. Given their high electrophilic character, they could thus form a novel ligand class, that is highly Lewis acidic σ-donor ligands.

Cationic transition metal complexes bearing two-coordinate Ge^{II} ligands, a number of which have been reported by Fillippou (Figure 1),[8] typically demonstrate linear L–Ge–M geometries in line with considerable M→Ge back donation, and hence a high degree of multiple bond character pertaining to triple bonds.[9] This, in turn, significantly reduces the Lewis acidity of the Ge centre. In these systems

[*] P. M. Keil, Dr. T. J. Hadlington
Fakultät für Chemie, Technische Universität München
Lichtenbergstraße 4, 85747 Garching (Germany)
E-mail: terrance.hadlington@tum.de
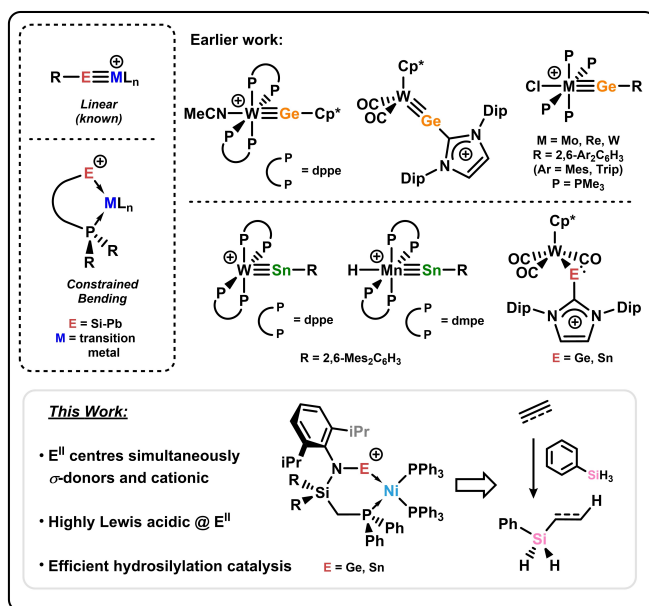
Figure 1. Known examples of cationic TM complexes bearing tetrylene E^{II} fragments (E = Ge, Sn), and the concept of "constrained bending" leading to a cationic E^{II} centre.

Angew. Chem. Int. Ed. **2022**, *61*, e202114143 (1 of 8)

© 2021 The Authors. Angewandte Chemie International Edition published by Wiley-VCH GmbH

the favourable formation of a triple bond will lead to the cationic charge residing largely on the TM centre or ancillary ligand, sequestering the Lewis acidity of the Ge centre. Whilst less explored, the bonding situation is similar for Sn. In rare cases for both Ge and Sn, multiple bonding is not favoured, and instead a metallotetrylene is formed (Figure 1),[8c] again lacking Lewis acidity at the tetryl centre due to the presence of a lone electron pair. It is surprising that the further reactivity of the described species has not yet been forthcoming, although there is a growing interest in the development of mixed-element systems for synergistic bond activation processes.[10]

To circumvent sequestration of reactivity at the tetryl centre, we sought novel *chelating* tetryliumylidene ligands with a geometrically constrained, sub-180° L–E–M angle (Figure 1), reducing M→E back-bonding and lending a high degree of Lewis acidity to the E centre. This should allow for strong electrophilic reactivity at this centre, hence opening a new vista in ligand design. Herein we describe such a chelating ligand system bearing E^{II} centres which act simultaneously as σ-donors and strong Lewis acids. The Lewis acidic nature of the E^{II} centres has been demonstrated through the binding of nucleophilic substrates such as ammonia, as well as fluoride abstraction from $[SbF_6]^-$. These novel systems have also been employed in the catalytic hydrosilylation of alkenes and alkynes, thus introducing a new ligand class for key transition metal catalysed processes.
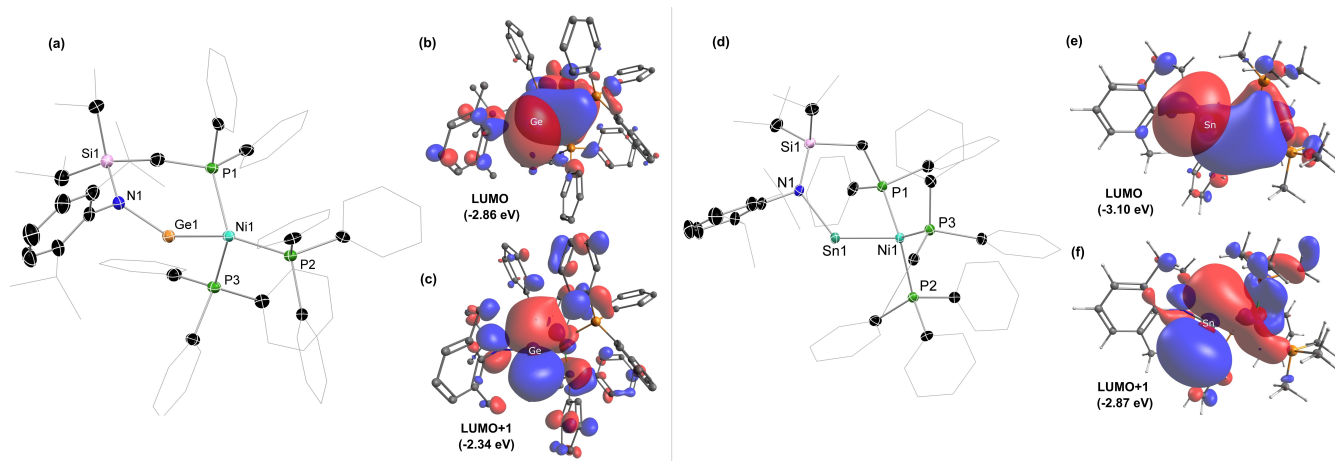
Results and Discussion

We recently reported the chloro-germylene Ni^0 complexes **3a** and **3b** (Scheme 1), which are accessible in gram-scale from phosphine-chelated chloro-germylenes, ^{PhPh}DippGeCl and ^{PhiP}-DippGeCl (^{PhPh}Dipp = {[Ph_2PCH_2Si(Ph)_2](Dipp)N}^-$; ^{PhiP}Dipp = {[Ph_2PCH_2Si(^iPr)_2](Dipp)N}^-$; Dipp = 2,6-$^iPr_2C_6H_3$).[11] Addition of NaBAr^F_4 ($Ar^F = 3,5$-(CF_3)_2C_6H_2$) to red-brown fluorobenzene solutions of **3a/b** led to an immediate colour change to
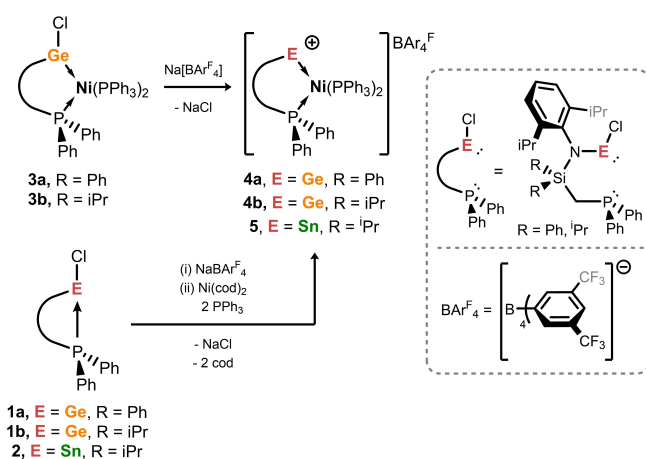
deep purple. For both species, in situ $^{31}P\{^1H\}$ NMR analysis indicated the formation of a single new compound, with a considerable increase in the $^2J_{PP}$ coupling of the two *P*-environments relative to **3** (e.g. for **3a**: $^2J_{PP} = 18.2$ Hz; for **4a**: $^2J_{PP} = 51.5$ Hz), concomitant with a shift towards coalescence of these signals (Figures S8 and S18 in the Supporting Information). Following work-up, deep purple-orange crystals of cationic species **4a/b** could be isolated, the ^1H and $^{31}P\{^1H\}$ NMR spectra of which match those for crude reaction mixtures. UV/Vis analyses of toluene solutions of **4b** show a blue-shift of the main absorbance from 362 nm ($\varepsilon = 9160$ L mol^{-1} cm^{-1}) in **3b** to 346 nm ($\varepsilon = 9870$ L mol^{-1} cm^{-1}) in **4b**, as well as a red shift and broadening of a second significant absorbance (486 nm, $\varepsilon = 2310$ L mol^{-1} cm^{-1}; Figure S24 in the Supporting Information). A TD-DFT analysis suggests that the major absorptions leading to the intense colour of **4b** are centred at 455 and 435 nm, and arise from HOMO→LUMO transitions which are essentially metal-to-ligand charge transfer processes (Figure S114 in the Supporting Information). The molecular structures of both **4a** (Figure S102 in the Supporting Information) and **4b** (Figure 2) reveal cationic single-centre ambiphile ligated Ni^0 complexes, containing two-coordinate Ge^{II} centres bound to Ni^0.[12] In **4b**, the Ni^0 centre pertains towards a trigonal-pyramidal geometry, the trigonal "base" formed by the three phosphine ligands (sum of [P–Ni–P] angles = 350.43°), capped by the germyliumylidene arm. The Ni–Ge–N angle of 132.96(1)° deviates considerably from linearity due to the chelation through the phosphine arm of the ligand scaffold, leading to considerable charge localization on Ge (see below), in stark contrast to previously reported cationic tetrylidyne transition-metal complexes, which contain multiply-bonded, linear L–Ge–M interactions, and hence bear considerable charge at M.[8] Reflecting this, the Ge–Ni distance in cationic **4b** ($d_{Ge-Ni} = 2.1908(9)$ Å) is essentially unchanged when compared to that in neutral **3b** ($d_{Ge-Ni} = 2.1877(7)$ Å), indicating a negligible increase in Ni→Ge back-bonding in forming the cationic complex. The frontier orbitals of cationic model complex $[4']^+$ (Figure 2; $[4']^+ = [^{PhMe}XylGe \cdot Ni(PPh_3)_2]^+$; $^{PhMe}Xyl = [(Ph_2PCH_2SiMe_2)(Xyl)N]^-$; $Xyl = 2,6$-Me_2C_6H_3$) calculated using DFT (Density Functional Theory) methods suggest that both the LUMO and LUMO+1 are high *p*-character orbitals localized at Ge (Figure 2 b and c), whilst the MBO (Mayer Bond Order) for the Ge–Ni interaction of 1.11 is similar to that for the related neutral model chloro-germylene complex **3'** (MBO = 1.13) and further related germylene complexes described herein (Table S3 in the Supporting Information).[13] An NBO analysis suggests that the largest contributions to the Ge–Ni interaction are Ge→Ni donation, with energies of 52.98 kcal·mol^{-1} and 95.45 kcal·mol^{-1} (Figures S104 and S105 in the Supporting Information). Three back-donation interactions can also be found, amounting to 64.55 kcal·mol^{-1} (Figures S106–S108 in the Supporting Information). This reiterates the notion that the Ge–Ni bonding interactions in **4a/b** are dominated by σ-donation, but also indicates that the chelate effect in these complexes does not entirely prevent Ni→Ge back-donation. We also note that, unlike a number of low-coordinate cationic main group species reported previously,[14] no arene contacts between flanking ligands in **4a/b** and the Ge^{II} in these species

Scheme 1. Synthesis of cationic complexes **4** and **5** through chloride abstraction from isolated Ni^0 complexes **3**, or a "one-pot" pot method utilising chloro-germylenes (**1**) or -stannylene (**2**).

Figure 2. a) The molecular structure of the cationic part of **4b**, with hydrogen atoms omitted and thermal ellipsoids at 30% probability. b) The LUMO and c) LUMO+1 of **[2']⁺**. d) The molecular structure of the cationic part of **5**, with hydrogen atoms omitted and thermal ellipsoids at 30% probability. e) The LUMO and f) the LUMO+1 of **[5'']⁺**. Selected distances [Å] and angles [°] for **4b**: Ni1–Ge1 2.1908(9), Ge1–N1 1.851(3); Ni1-Ge1-N1 133.0(1), P1-Ni1-P2 123.42(4), P1-Ni1-P3 117.28(4), P2-Ni1-P3 109.73(4). Selected distances [Å] and angles [°] for **5**: Ni1–Sn1 2.2.4024(9), Sn1–N1 2.068(5); Ni1-Sn1-N1 124.3(1), P1-Ni1-P2 125.51(6), P1-Ni1-P3 118.42(6), P2-Ni1-P3 111.48(6).

are apparent in their solid-state structures,[15] but N→Ge donation does aid in stabilizing the Ge^{II} centre in these complexes (viz. HOMO-21, Figure S111 in the Supporting Information).[16]

As cationic complexes **4a/b** are diamagnetic, and so formally d^{10} at Ni, they are best described as bearing a cationic one-coordinate germylene in the coordination sphere of neutral Ni^0, and as such represent a novel ligand binding motif when compared with any previously reported species.[7,17] We were thus curious as to whether the related Sn^{II} complex could be accessed, given that such complexes for this element are also unknown. Sn^{II} derivatives of **3a/b** proved unstable, and could not be isolated. However, the one-pot reaction between first the chloro-stannylene **2** and NaBAr$^F_4$, with subsequent addition of Ni(cod)$_2$ and 2 equivalents PPh$_3$ led to deep purple reaction mixtures, similar to dissolved **4a/b**. ^{31}P{^{1}H} NMR spectroscopic analysis of crude reaction mixtures suggested remarkably clean conversion to a single product, with a shift and splitting pattern mirroring that for **4b**. Filtration, removal of volatiles, and addition of small amounts of pentane led to a large crop of dark purple crystals, an X-ray diffraction analysis of which revealed the formation of the cationic stannylene Ni^0 complex **5** (Figure 2d). The high yield (78%) and expedient nature of this reaction led us to synthesise Ge^{II} complex **4b** in a similar manner, giving access to this species in 80% yield.

Due to the larger radius of Sn, the Sn–Ni distance in **5** ($d_{Sn-Ni} = 2.4024(9)$ Å) is elongated relative to the Ge–Ni interaction in **4b** ($d_{Ge-Ni} = 2.1908(9)$ Å). The internal N–Sn–Ni angle of 124.3(1)° is slightly contracted compared to the Ni–Ge–N angle in **4b** most likely due to reduced *sp*-mixing in the Sn derivative, as in known more broadly for the heavier tetrylenes.[18] The Ni^0 centre in **5**, is coordinated in a near trigonal planar fashion by its three phosphine ligands (sum of [P–Ni–P] angles = 355.41°), and is capped by the Sn^{II} ligand centre to form a distorted trigonal-pyramidal geometry at

nickel. The ^{119}Sn NMR spectrum of **5** presents a broad peak at $\delta = 1342$ ppm, and so reveals no $^2J_{SnP}$ coupling information. As for **4b**, a computational NBO analysis of model complex **[5']⁺** is indicative of both Sn→Ni donation (32.59 kcal mol^{-1}) and back donation from Ni (43.75 kcal mol^{-1}), both of these interactions being weaker than for the comparable Ge system and leading to a decreased MBO of 0.79 for this interaction. Both the LUMO and LUMO+1 represent vacant orbitals at Sn^{II} (Figure 2e and f), again in keeping with the Ge derivative, suggesting this centre too should bear a considerable degree of Lewis acidity.

Metrical and electronic parameters in **4a/b** and **5** suggested to us that the electrophilicity at the Ge^{II}/Sn^{II} centres should be high when compared with related multiply-bonded or metallotetrylene species. The first evidence for this was given by the coordination of DMAP to the Ge^{II} centre in **4b**, leading to brown-purple reaction mixtures, from which deep blue-purple X-ray quality crystals could be isolated. The molecular structure of **4b·DMAP** (Figure 3) confirms binding at Ge^{II}, with coordination in the N–Ge-Ni plane forming a trigonal-planar Ge centre (sum of angles = 359.45°). Relative to **4b**, only a small increase in the Ni–Ge distance is observed ($d_{Ge-Ni} = 2.228(1)$ Å). Adduct **4b·DMAP** is unstable in solution, giving complex ^{31}P{^{1}H} NMR spectra upon dissolution of pure crystalline material at ambient temperature. Dissolving samples at −80°C in D$_8$-THF, however, allows for the observation of ^{31}P{^{1}H} NMR spectra which contain three signals pertaining to the three phosphine ligands (Figure S50 and S51 in the Supporting Information), presumably separated due to "freezing out" of ligand exchange/rotation processes. Slow warming leads to initial broadening of the signals, up to −20°C, followed by the appearance of a number of new resonances due to complex decomposition.

Addition of an excess of NH$_3$ to solutions of **4a** led to the clean formation of a single new species as ascertained by
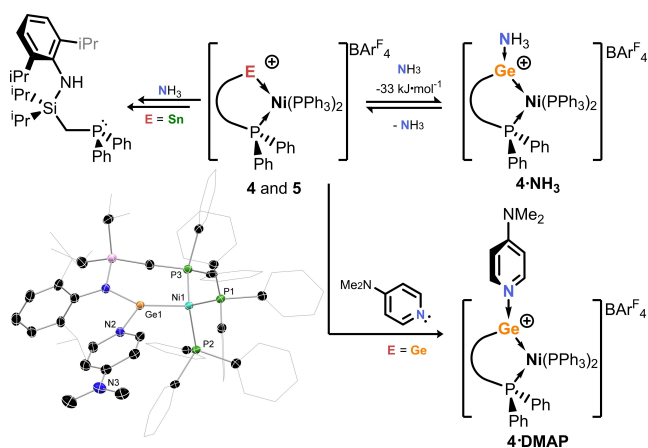
Figure 3. Reactivity of cationic **4** and **5** towards NH_3 and DMAP. Below: The molecular structure of **4a·DMAP**, with hydrogen atoms eliminated and thermal ellipsoids at 30% probability. Selected distances [Å] and angles [°] for **4a·DMAP**: Ge1–Ni1 2.228(1), Ge1–N1 1.871(3), Ge1–N2 2.114(4), P1–Ni1 2.259(1), P2–Ni1 2.217(1), P3–Ni1 2.258(2); N1-Ge1-N2 101.0(1), Ni1-Ge1-N1 133.5(1), Ni1-Ge-1-N2 124.97(9).

$^{31}P\{^1H\}$ NMR spectroscopy, in the formation of orange solutions. The $^{31}P\{^1H\}$ NMR spectra of these samples show a considerably reduced $^2J_{PP}$ coupling value akin to those in chloro-germylene Ni^0 complex **3a**, i.e. with a three-coordinate Ge^{II} centre. Addition of between 0.5 and 3 equivalents of NH_3 leads to the gradual formation of the same species, whilst removal of volatiles in vacuo, followed by redissolving the residue regenerates the starting material, **4a** (Figure 4a).
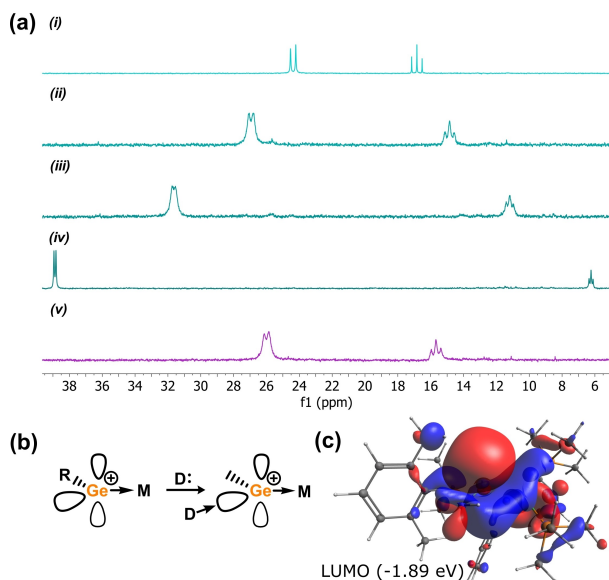
Figure 4. a) $^{31}P\{^1H\}$ NMR spectra of i) compound **4a**, ii) **4a** + 0.5 equiv NH_3, iii) **4a** + 1 equiv NH_3, iv) **4a** + 3 equiv NH_3, and v) removal of all volatiles followed by redissolving in C_6H_5F (all other spectra also as C_6H_5F solutions). b) A schematic representation of the LUMO and LUMO + 1 in **4a/b**, and the formation of an in-plane donor–acceptor complex (R = anionic ligand; M = transition metal, D = Lewis basic donor). c) The LUMO of NH_3 adduct of $[4'']^+$.

Resonances for solutions treated with 0.5 and 1 equivalent of NH_3 show signal broadening, which we hypothesise is due to a rapid equilibrium between **4a** and the ammonia adduct, **4a·NH₃**. Attempts to crystallise this adduct were unsuccessful, leading only to the isolation of **4a**.[19] Nevertheless, the above observations, alongside the favourable DFT-derived binding energy of NH_3 to the Ge^{II} centre in $[4']^+$ ($\Delta G = -33$ kJ mol^{-1}), give strong evidence for a reversible ammonia binding process. We also note that the DFT-optimized geometry of $[4']^+ \cdot NH_3$ shows in-plane binding, akin to that observed structurally for **4a·DMAP**, with one remaining vacant *p*-orbital at Ge^{II} (Figure 4b and c).[20]

To further investigate the reversibility in ammonia binding, the previously reported amido-germylene Ni^0 complex **6b** (Scheme 2) was reacted with the oxonium salt, $HBAr^F_4$ ($HBAr^F_4 = [(Et_2O)_2H][BAr^F_4]$), in order to protonate the NH_2 group in the loss of NH_3. This reaction proceeds remarkably cleanly, forming deep purple solutions with ^1H and $^{31}P\{^1H\}$ NMR spectra matching samples of **4b** (Figure S27 in the Supporting Information). The facility of this reaction was further extended, in addition of $HBAr^F_4$ to the hydroxy-germylene Ni^0 complex **7b**, as well as to the unprecedented hydrido-germylene Ni^0 complexes **8a** and **8b**, synthesized through salt-metathesis of chloro-germylene complexes **3a/b** with Li[$^sBu_3BH$] (Scheme 2, Figure 5). The former presumably leads to initial formation of the adduct **4b·OH₂**, which eliminates H_2O to form the free cation **4b** (Figure S28). The related reaction is considerably clearer for the hydride complexes **8a** and **8b**. The ^1H NMR spectra for these species show considerably down-field shifted Ge-H resonances when compared with known Ge^{II} hydride species, indeed more so than any Ge^{II} hydride reported to date,[21] indicative of the electron-deficient nature of the Ge^{II} centres in **8a** and **8b**.[22] This clear down-field shift, alongside their characteristic doublet-of-triplets splitting pattern (e.g. for **8b**: $\delta = 11.17$ ppm, $^3J_{HP} = 37.7$, 6.5 Hz; Figure S23 in the Supporting Information) makes the disappearance of these
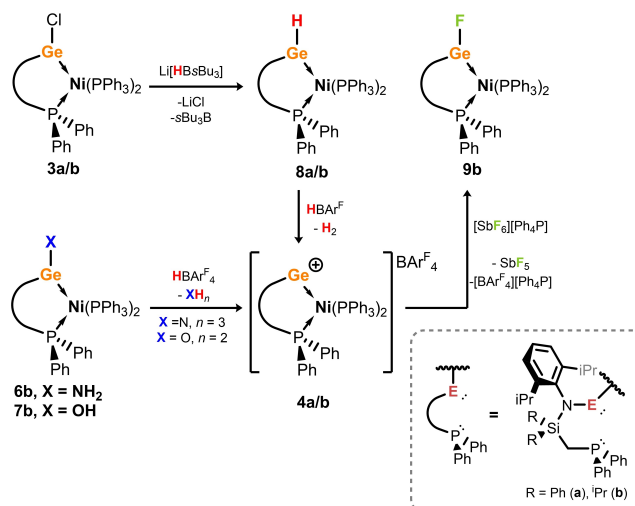
Scheme 2. Synthesis of hydrido-germylene complexes **8 a/b**, conversion of complexes **6b**, **7b**, and **8a/b** to cationic **4a/b** with loss of NH_3, H_2O, and H_2, respectively, and fluoride abstraction from [SbF_6]$^-$ by **4a/b**.
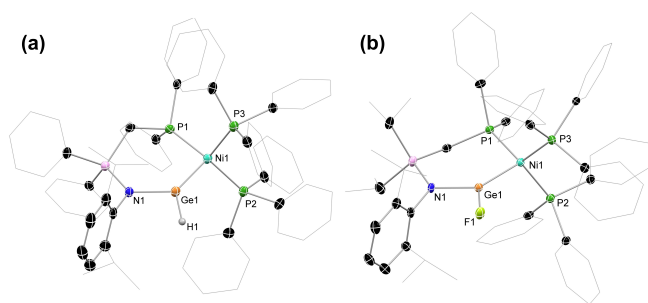
Figure 5. Molecular structures of a) **8a** and b) **9b**, with hydrogen atoms (aside from the H1 in **8a**) omitted, and thermal ellipsoids at 30% probability. Selected distances [Å] and angles [°] for **8a**: Ge1–Ni1 2.228(2), Ge1–H1 1.64(6), Ge1–N1 1.881(7); N1-Ge1-Ni1 127.7(2), P1-Ni1-Ge1 100.22(6). For **9b**: Ni1–Ge1 2.1758(8), Ge1–N1 1.852(3), Ge1–F1 1.798(2); Ni1-Ge1-N1 133.03(9), F1-Ge1-N1 97.7(1), Ni1-Ge1-F1 129.18(7), P1-Ni1-Ge1 98.33(3).

signals quite clear. Addition of HBAr$^F_4$ to C_6D_6 solutions of **8a** and **8b** eliminates H_2, observable in the ^1H NMR spectra of reaction mixtures as a singlet at $\delta = 4.47$ ppm (Figures S15, S16, S25, and S26 in the Supporting Information), with concomitant disappearance of the distinct Ge-*H* resonances. As a whole, this set of experiments firstly demonstrates the reversible binding of NH_3 (and H_2O) to cations **4a** and **4b**, whilst also giving a range of synthetic routes to these novel cationic complexes which we are currently exploring in related main-group systems.

We also sought to employ chemical probes to access the Lewis acidity of **4a/b** and **5** (e.g. Gutmann–Beckett,[23] Childs,[24] and nitrile-binding methods).[25] In all cases, extreme signal broadening or divergent chemical reactivity was observed, a common issue with such methods in more complex chemical systems.[26] Given that the benchmark for Lewis superacidity is the FIA (FIA = Fluoride Ion Affinity) of SbF_5,[27] it so follows that F$^-$ abstraction from the $[SbF_6]^-$ anion indicates a high degree of Lewis acidity, pertaining to Lewis superacidity. It was thus very promising to find that cation **4b** reacts with $[SbF_6][PPh_4]$ in the formation of neutral fluoro-germylene Ni^0 complex **9b**, SbF_5, and $[BAr^F_4][PPh_4]$ (Scheme 2).[28] The molecular structure of **9b** is isostructural to chloride derivative **3b** in the solid state (Figure 5), showing a doublet in its ^{19}F NMR spectrum. The $^{31}P\{^1H\}$ NMR spectrum of this compound indicates that only the chelating P-arm couples with the Ge-*F* centre, presenting as a doublet of triplets ($^2J_{PP} = 16$ Hz; $^3J_{PF} = 108$ Hz), and a doublet for the two Ph$_3$P ligands (Figure S57 in the Supporting Information). The instability of the stannylene Ni^0 complex ^{PhiP}DippSnCl·Ni(PPh$_3$)$_2$ negates the isolation of a fluoro-stannylene complex through reaction of **5** with $[SbF_6][PPh_4]$, although this reaction does produce SbF_5 and $[BAr^F_4][PPh_4]$, suggesting fluoride abstraction does indeed occur (Figure S36 and S37 in the Supporting Information).

The calculated FIA and HIA (HIA = Hydride Ion Affinity) values have become a standard measure of the hard and soft Lewis acidity of a system, respectively,[27,29] whilst more recently the AA (Ammonia Affinity) and WA (Water Affinity) have been employed to take account for steric

effects.[30] This set of affinities thus gives a multidimensional view of the Lewis acidity of electrophiles accounting for hard and soft Lewis acidity (i.e. FIA and HIA), as well as steric effects (i.e. AA and WA). These values were calculated for the Ge^{II} systems **[4']$^+$** and **[4'']$^+$** ([4'']$^+$ = [^{PhMe}XylGe·Ni(PMe$_3$)$_2$]$^+$), and for the Sn^{II} system **[5'']$^+$**, at the ωB97XD/def2SVP (Ni, Ge, Sn: def2TZVPP) level of theory in the gas phase.[31] Reference values were also calculated for SbF_5 and BCF (BCF = B(C$_6$F$_5$)$_3$) at the same level of theory due to the experimentally observed reaction between $[SbF_6]^-$ and **4b**, and BCF being a common reference point for Lewis acidity, which were found to correlate well with literature values obtained with more intensive computational methods (Table 1). Values were additionally calculated for the known $[Mes_3Si]^+$ system, as an established cationic strong Lewis acid.[32] Both the FIA (636 kJ mol^{-1}) and HIA (639 kJ mol^{-1}) values for **[4'']$^+$** are greater than those for SbF_5 (FIA: 495 kJ mol^{-1}; HIA: 571 kJ mol^{-1}) and BCF (FIA: 457 kJ mol^{-1}; HIA: 493 kJ mol^{-1}), corroborating the experimental observation that **4b** abstracts F$^-$ from $[SbF_6]^-$, and further supporting the notion of a high degree of Lewis acidic character in this complex. Similarly high FIA and HIA values are observed for the model Sn^{II} complex **[5'']$^+$** (FIA: 618 kJ mol^{-1}; HIA: 622 kJ mol^{-1}). The favourable AA (24 kJ mol^{-1}) and WA (17 kJ mol^{-1}) values for **[4'']$^+$** are in keeping with the observed binding of NH_3 to the Ge^{II} centre in **4a**. Still, comparing to the well-established cationic Lewis acid $[Mes_3Si]^+$, which has considerably higher FIA, HIA, AA and WA values (Table 1), it is clear that potential Lewis acidity in **4a/b** and **5** is quenched to some degree, most likely through the aforementioned N→E donation. The inclusion of more sterically demanding Ph groups at the R$_3$P ligands in **[4']$^+$** in fact improves the AA value (33 kJ mol^{-1}), which we postulate is due to increased dispersion interactions. Notably, however, these AA and WA values are considerably lower than those for SbF_5, BCF, and $[Mes_3Si]^+$, and perhaps reflect the considerable steric congestion in **4b** relative to those classic Lewis acids. Still, this collection of calculated values, alongside the experimental observations of DMAP and ammonia binding, and fluoride abstraction, give strong evidence that **4b** can behave as a universal Lewis acid, aiding in defining a new ligand class in the chelating cationic single-centre ambiphiles.

Table 1: DFT-derived ion fluoride and hydride ion affinities (FIA and HIA, respectively) and ammonia and water affinities (AA and WA, respectively).[a]

Lewis Acid (LA)	FIA	HIA	AA[b]	WA[b]
[4']$^+$	639	643	33	11
[4'']$^+$	636	639	24	17
[5'']$^+$	618	622	16	11
B(C$_6$F$_5$)$_3$	457 (448)[c]	493 (484)[d]	100 (122)[d]	39 (54)[d]
SbF$_5$	495 (496)[c]	571 (535)[d]	143 (163)[d]	84 (99)[d]
[Mes$_3$Si]$^+$	841	859	50	57

[a] at the ωB97XD/def2-SVP(Ni,Ge,Sn: def2-TZVPP) level. [b] AA and WA values are calculated as free energies. [c] Values in parentheses are taken from Ref. [29c]. [d] Values in parentheses are taken from Ref. [30].

To probe the tetrylene-like reactive character in **4a/b** and **5** we sought to observe oxidative chemistry at their E^{II} centres, reactivity which has been observed for low-coordinate tetrylene systems in the past.[33] Ethylene and diphenylacetylene, which may be expected to undergo [2+1] cycloaddition processes, showed no reaction. Silanes and boranes, which may undergo oxidative cleavage, also showed no reaction.[34] These observations give further evidence of the formal donor nature of the E^{II} centres in these complexes. Remarkably, however, cationic complexes **4b** and **5** proved to be active catalysts for the hydrosilylation of alkynes and alkenes. Given the importance of hydrosilylation in both an academic and industrial setting,[35] alongside the need for the development of systems utilizing benign and abundant elements,[36] this is an exciting finding. In an initial test, a mixture of 1 mol% **4b**, PhCCPh, and PhSiH$_3$ led to selective formation of *trans*-(Ph)(H)C=C-(SiH$_2$Ph)(Ph), with 68% conversion at 60°C after 16 h. Increasing catalyst loading to 2.5 mol% led to full conversion after 18 h. Screening a number of alkynes under similar conditions (Table 2) demonstrates this protocol can be extended, allowing hydrosilylation of even the bulky Me$_3$SiCCMe. In all cases, the only species observable in the ^{31}P{^{1}H} NMR spectra was **4b**, suggesting that this is the catalyst resting state. Sn^{II} complex **5** also proved to be an active catalyst for alkyne hydrosilylation, generally showing an improved activity relative to **4b** as exemplified by the described reaction of PhCCPh being complete in 4 h, comparing to 18 h for similar conditions using **4b**.

The scope of the reaction was then extended to alkenes. This was initially optimized for 1-hexene, which surprisingly seemed to proceed much more rapidly than for alkynes under similar conditions (Table 3). Addition of PhSiH$_3$ to 1-hexene in the presence of 2.5 mol% **4b** gave 90% consumption of PhSiH$_3$ in forming the *anti*-Markonikov 1-silylhexane after 12 h at ambient temperature, and 4 h at 60°C. As a side

Table 2: The hydrosilylation of alkynes catalyzed by **4b** or **5**.[a]

Catalyst	R, R′	t	Conversion, [%][b] (A:B)
4b	Ph, Ph	18 h	99
4b	Ph, Me	3 h	98 (1:1.3)
4b	SiMe$_3$, Me	72 h	74 (1:0)
4b	^{n}Pr, ^{n}Pr	72 h	64
5	Ph, Ph	4 h	98
5	Ph, Me	5 h	93 (1:1.4)
5	SiMe$_3$, Me	72 h	86 (1:0)
5	^{n}Pr, ^{n}Pr	77 h	77
–[c]	Ph, Me	24	0

[a] Conducted in 0.4 mL C$_6$D$_6$ in gas-tight NMR tubes, with 1.0 equiv of alkyne. [b] Determined by relative integration of Si-*H* signals in ^{1}H NMR spectra of reaction mixtures, and based upon consumption of PhSiH$_3$ starting material.; [c] Carried out in the absence of catalyst.

Table 3: Optimisation of 1-hexene hydrosilylation using complex **4b**.[a]

Catalyst loading (mol%)	T [°C][b]	t [h]	Conversion [%][c]	Ratio P:A[d]	Ratio P:B[e]
1	RT	4	75	209:1	3.8:1
1	RT	48	94	72:1	4.5:1
2.5	RT	4	80	203:1	5.9:1
2.5	RT	12	90	98:1	6.5:1
5	RT	4	76	126:1	4.2:1
5	RT	12	91	65:1	4.8:1
1	60	4	88	35:1	4.7:1
2.5	60	4	90	34:1	5.0:1
5	60	4	91	23:1	5.5:1
5	60	90	99[f]	–	–(2.7:1)[g]
–[h]	60	24	0	–	–
2.5[i]	RT	12	17	–	–
2.5[j]	RT	0.5	65	–	5.5:1
		12	80	–	5.5:1

[a] Conducted in 0.4 mL C$_6$D$_6$ in gas-tight NMR tubes. [b] RT defined as 22°C. [c] Determined by relative integration of Si-*H* signals in ^{1}H NMR spectra of reaction mixtures, and based upon ratio of PhSiH$_3$ to **P**. [d] Determined by integration of Si-*H* peaks for **P** and **A** in ^{1}H NMR spectra of crude reaction mixtures. [e] Determined by integration of the Si-*H* peak for **P** and alkenyl C−*H* peaks for **B** in ^{1}H NMR spectra of crude reaction mixtures. [f] Conducted in the absence of PhSiH$_3$, showing full isomerisation to **B**. [g] Ratio in parentheses refers to the *cis*:*trans* ratio for the formed 2-hexene. [h] Carried out in the absence of catalyst. [i] Ni(cod)$_2$/PPh$_3$ (1:4) was employed as the catalyst. [j] Complex **3b** used as the catalyst. N.B. Catalytic activity is not hampered by the addition of 0.1 mL Hg.

reaction, up to 17% of the 1-hexene substrate undergoes isomerization to a mixture of *cis*- and *trans*-2-hexene, with this process being more prominent at lower catalyst loadings. In the absence of PhSiH$_3$, full isomerization of 1-hexene to 2-hexene is achieved (5 mol%, 60°C, 80 h), a promising observation for the future scope of this catalytic system. The undesirable catalyzed redistribution of PhSiH$_3$ to Ph$_2$SiH$_2$ (and presumably SiH$_4$) is also observed, exacerbated at higher temperatures and catalyst loadings. To assess the importance of the cationic single-centre ambiphile ligand in the catalytic activity of **4b**, Ni(cod)$_2$/PPh$_3$ (1:4 mixture) was employed as a catalyst, showing a low conversation of 17% at 2.5 mol% loading after 12 h (Figure S95 in the Supporting Information), suggesting that the Ge^{II} centre indeed imparts activity in our system. Utilising the neutral chloro-germylene complex **3b** as a catalyst in fact led to an extremely high initial activity, reaching 65% after 30 min at ambient temperature. This catalyst proved highly unstable, however, and had largely decomposed after this short time, as shown by ^{31}P NMR spectroscopy, with little further conversion after 12 h (Figures S96–S98 in the Supporting Information). These observations are somewhat surprising; whilst they indicate the benefits of the presence of the germylene/germyliumylidene species for catalytic turnover, the increased activity and instability in the neutral system certainly warrants further investigation in future studies.

Extending this protocol to a range of alkenes showed selective conversion to the *anti*-Markovnikov 1-silylalkanes (Table 4). In the majority of cases mono-insertion products are favoured (i.e. yielding PhRSiH$_2$); for ethylene, double-insertion leading to the formation of PhEt$_2$SiH is prominent when the reaction is conducted at 60°C, and is complete after just 1 h. Conducting the same reaction at room temperature leads to selective formation of the mono-insertion product, PhEtSiH$_2$. The related Sn^{II} system, **5**, was also screened as a catalyst in the hydrosilylation of alkenes (Table 4). In contrast to the increased reaction rates for the Sn^{II} system in alkyne hydrosilylation, alkene hydrosilylation is considerably slower, whilst the competing isomerization reaction for 1-hexene is seemingly more pronounced. The hydrosilylation of ethylene with **5** is selective for the formation of the mono-insertion product at 60°C, in contrast to the Ge^{II} system. In light of these differences, we are presently developing further ligand systems, to conduct an in-depth mechanistic study to determine any involvement of the developed cationic ligands in the catalytic regime. Finally, whilst the activities reported here are rather modest when compared with reported Ni hydrosilylation catalysts,[14] we note that this is the first demonstration of the utility of our novel ligand class in catalysis, opening the door for future developments.

Table 4: Hydrosilylation of terminal alkenes with complexes **4b** and **5**.[a]

Catalyst	Catalyst loading (mol%)	R	*t*	Conversion [%][b]
4b	2.5	H	1 h	99[c]
4b	2.5	H	24 h	97[d]
4b	0.5	CyCH$_2$	4 h	69
4b	1	CyCH$_2$	1 h	92
4b	2.5	CyCH$_2$	20 min	99
4b	0.5	SiMe$_3$	4 h	62
4b	1	SiMe$_3$	1 h	85
4b	2.5	SiMe$_3$	20 min	90
4b	2.5	*p*-CF$_3$C$_6$H$_4$CH$_2$	17 h	75
4b	2.5	PhCH$_2$	72 h	65
4b	2.5	^{t}Bu	72 h	44
4b	2.5[e]	^{n}Pr	24 h	16
5	2.5	^{n}Pr	48 h	71
5	2.5	H	1 h	99
5	2.5	CyCH$_2$	48 h	59
5	2.5	SiMe$_3$	20 h	86
5	2.5	*p*-CF$_3$C$_6$H$_4$CH$_2$	24 h	79
5	2.5	PhCH$_2$	72 h	43
5	2.5	^{t}Bu	72 h	20

[a] Conducted in 0.4 mL C$_6$D$_6$ in gas-tight NMR tubes, with 1.3 equiv of alkene. [b] Determined by relative integration of Si-*H* signals in ^{1}H NMR spectra of reaction mixtures, and based upon consumption of PhSiH$_3$ starting material. [c] The only product formed under these conditions is PhEt$_2$SiH. [d] The reaction was carried out at RT. [e] The reaction was carried out in the presence of 250 mol% PPh$_3$.

Conclusion

We have developed a chelating ligand system based upon reactive low-coordinate cationic E^{II} centres (E = Ge, Sn), which, due to the electronic ground state of singlet tetrylenes, act as σ-donor ligands whilst remaining highly electrophilic. This unique ligand system has been employed in the formation of Ni^0 complexes **4a/b** and **5**, in which the binding of Lewis bases, namely 4-*N,N*-dimethylaminopyridine and ammonia, can readily occur at the E^{II} centre. Formation of the described cationic complexes is also possible through protonation of amido-, hydroxy-, and hydrido-germylene Ni^0 complexes **6–8**, in the loss of NH$_3$, H$_2$O, and H$_2$, respectively. Remarkably, the E^{II} centres in these Ni^0 complexes even pertain towards Lewis superacidity, capable of abstracting the fluoride ion from [SbF$_6$]$^-$ in the formation of fluoride-germylene complex **9**. The capacity for these complexes to affect catalysis has also been demonstrated; the hydrosilylation of alkenes and alkynes, as well as the isomerization of 1-hexene to 2-hexene, is reported. As a whole, this collection of results thus demonstrates the utility of single-centred ambiphilicity in readily accessible low-valent main group ligands, the further reactivity of which we are presently fervently pursuing, towards defining multi-centred synergistic bond activation processes and catalysis.

Conflict of Interest

The authors declare no conflict of interest.

Data Availability Statement

The data that support the findings of this study are available from the corresponding author upon reasonable request.

[1] a) Y. Mizuhata, T. Sasamori, N. Tokitoh, *Chem. Rev.* **2009**, *109*, 3479–3511; b) G. Frenking, R. Tonner, S. Klein, N. Takagi, T. Shimizu, A. Krapp, K. K. Pandey, P. Parameswaran, *Chem. Soc. Rev.* **2014**, *43*, 5106–5139; c) J. Baumgartner, C. Marschner, *Rev. Inorg. Chem.* **2014**, *34*, 119–152.

Angew. Chem. Int. Ed. **2022**, *61*, e202114143 (7 of 8)

© 2021 The Authors. Angewandte Chemie International Edition published by Wiley-VCH GmbH

[2] a) *Metal carbenes in organic synthesis* (Ed.: K. H. Dötz), Springer, Berlin, **2004**; b) K. H. Dötz, J. Stendel, Jr., *Chem. Rev.* **2009**, *109*, 3227–3274.

[3] a) M. N. Hopkinson, C. Richter, M. Schedler, F. Glorius, *Nature* **2014**, *510*, 485–496; b) *N-Heterocyclic Carbenes in Transition Metal Catalysis* (Ed.: F. Glorius), Springer, Berlin, **2007**; c) V. Nesterov, D. Reiter, P. Bag, P. Frisch, R. Holzner, A. Porzelt, S. Inoue, *Chem. Rev.* **2018**, *118*, 9678–9842.

[4] P. Jutzi, *Angew. Chem. Int. Ed. Engl.* **1975**, *14*, 232–245; *Angew. Chem.* **1975**, *87*, 269–283.

[5] For key examples of multiply-bonded germylene-TM complexes, see: a) W.-W. du Mont, L. Lange, S. Pohl, W. Saak, *Organometallics* **1990**, *9*, 1395–1399; b) P. G. Hayes, R. Waterman, P. B. Glaser, T. D. Tilley, *Organometallics* **2009**, *28*, 5082–5089; c) M. C. Lipke, F. Neumeyer, T. D. Tilley, *J. Am. Chem. Soc.* **2014**, *136*, 6092–6102; d) A. C. Filippou, D. Hoffmann, G. Schnakenburg, *Chem. Sci.* **2017**, *8*, 6290–6299.

[6] L. Pu, B. Twamley, S. T. Haubrich, M. M. Olmstead, B. V. Mork, R. S. Simons, P. P. Power, *J. Am. Chem. Soc.* **2000**, *122*, 650–656.

[7] J. D. Queen, A. C. Phung, C. A. Caputo, J. C. Fettinger, P. P. Power, *J. Am. Chem. Soc.* **2020**, *142*, 2233–2237.

[8] a) A. C. Filippou, A. I. Philippopoulos, P. Portius, G. Schnakenburg, *Organometallics* **2004**, *23*, 4503–4512; b) A. C. Filippou, A. Barandov, G. Schnakenburg, B. Lewall, M. van Gastel, A. Marchanka, *Angew. Chem. Int. Ed.* **2012**, *51*, 789–793; *Angew. Chem.* **2012**, *124*, 813–817; c) A. C. Filippou, U. Chakraborty, G. Schnakenburg, *Chem. Eur. J.* **2013**, *19*, 5676–5686; d) Y. N. Lebedev, U. Das, G. Schnakenburg, A. C. Filippou, *Organometallics* **2017**, *36*, 1530–1540.

[9] Related neutral complexes are known for germanium, formally tetrylidyne complexes, as are a handful of related singly-bonded complexes which are better described as metallo-tetrylenes. For examples of the former, see refs [6,7], and: a) A. C. Filippou, A. I. Philippopoulos, P. Portius, D. U. Neumann, *Angew. Chem. Int. Ed.* **2000**, *39*, 2778–2781; *Angew. Chem.* **2000**, *112*, 2881–2884; b) A. C. Filippou, K. W. Stumpf, O. Chernov, G. Schnakenburg, *Organometallics* **2012**, *31*, 748–755. For examples of the latter, see ref [6] and c) R. S. Simons, P. P. Power, *J. Am. Chem. Soc.* **1996**, *118*, 11966–11967; d) H. Lei, J.-D. Guo, J. C. Fettinger, S. Nagase, P. P. Power, *Organometallics* **2011**, *30*, 6316–6322; e) J. Hicks, T. J. Hadlington, C. Schenk, J. Li, C. Jones, *Organometallics* **2013**, *32*, 323–329.

[10] R. J. Somerville, J. Campos, *Eur. J. Inorg. Chem.* **2021**, 3488–3498.

[11] P. M. Keil, T. Szilvasi, T. J. Hadlington, *Chem. Sci.* **2021**, *12*, 5582–5590.

[12] Deposition Numbers 2114015 (for **2**), 2099955 (for **4a**), 2099956 (for **4b**), 2114016 (for **5**), 2099957 (for **4a·DMAP**), 2099958 (for **8a**), 2099959 (for **8b**), and 2099960 (for **9b**) contain the supplementary crystallographic data for this paper. These data are provided free of charge by the joint Cambridge Crystallographic Data Centre and Fachinformationszentrum Karlsruhe Access Structures service www.ccdc.cam.ac.uk/structures.

[13] Value for the MBO of **1′** taken from ref. [9].

[14] a) S. Hino, M. Brynda, A. D. Philips, P. P. Power, *Angew. Chem. Int. Ed.* **2004**, *43*, 2655–2658; *Angew. Chem.* **2004**, *116*, 2709–2712; b) J. Li, C. Schenk, F. Winter, H. Scherer, N. Trapp, A. Higelin, S. Keller, R. Pöttgen, I. Krossing, C. Jones, *Angew. Chem. Int. Ed.* **2012**, *51*, 9557–9561; *Angew. Chem.* **2012**, *124*, 9695–9699.

[15] Close contacts are considered to be those with a distance less than the sum of the van der Waals radii of the two elements.

[16] a) J. Li, C. Schenk, C. Goedecke, G. Frenking, C. Jones, *J. Am. Chem. Soc.* **2011**, *133*, 18622–18625; b) T. J. Hadlington, B.

[17] To the best of our knowledge, the only reported examples of related species, that is cationic complexes in which a non-linear L–E–M interaction is observed, can be found in the following. However, these are better described as metallotetrylenes, without significant charge localization at the E centre (E = Ge, Sn). a) A. C. Filippou, B. Baars, O. Chernov, Y. N. Lebedev, G. Schnakenburg, *Angew. Chem. Int. Ed.* **2014**, *53*, 565–570; *Angew. Chem.* **2014**, *126*, 576–581; b) K. Inomata, T. Watanabe, H. Tobita, *J. Am. Chem. Soc.* **2014**, *136*, 14341–14344.

[18] a) R. C. Fischer, P. P. Power, *Chem. Rev.* **2010**, *110*, 3877–3923; b) P. P. Power, *Nature* **2010**, *463*, 171–177.

[19] Similar results were obtained when using **4b**.

[20] We note that attempts to extend this reaction to the Sn^{II} system **5** led only to the formation of protonated ligand, ^{PhiP}DippH.

[21] M. M. D. Roy, A. A. Omaña, A. S. S. Wilson, M. S. Hill, S. Aldridge, E. Rivard, *Chem. Rev.* **2021**, *121*, 12784–12965.

[22] T. J. Hadlington, M. Driess, C. Jones, *Chem. Soc. Rev.* **2018**, *47*, 4176–4197.

[23] U. Mayer, V. Gutmann, W. Gerger, *Monatsh. Chem.* **1975**, *106*, 1235–1257.

[24] R. F. Childs, D. L. Mulholland, A. Nixon, *Can. J. Chem.* **1982**, *60*, 809–812.

[25] S. Künzler, S. Rathjen, A. Merk, M. Schmidtmann, T. Müller, *Chem. Eur. J.* **2019**, *25*, 15123–15130.

[26] a) J. Pahl, S. Brand, H. Elsen, S. Harder, *Chem. Commun.* **2018**, *54*, 8685–8688; b) M. Schorpp, I. Krossing, *Chem. Sci.* **2020**, *11*, 2068–2076.

[27] L. O. Müller, D. Himmel, J. Stauffer, G. Steinfeld, J. Slattery, G. Santiso-Quiñones, V. Brecht, I. Krossing, *Angew. Chem. Int. Ed.* **2008**, *47*, 7659–7663; *Angew. Chem.* **2008**, *120*, 7772–7776.

[28] Fluoride complex **6** can also be independently synthesized through reaction of Me$_3$SnF with chloride complex **3b**.

[29] a) I. A. Koppel, P. Burk, I. Koppel, I. Leito, T. Sonoda, M. Mishima, *J. Am. Chem. Soc.* **2000**, *122*, 5114–5124; b) L. Greb, *Chem. Eur. J.* **2018**, *24*, 17881–17896; c) P. Erdmann, J. Leitner, J. Schwarz, L. Greb, *ChemPhysChem* **2020**, *21*, 987–994; d) A. Hermannsdorfer, M. Driess, *Angew. Chem. Int. Ed.* **2021**, *60*, 13656–13660; *Angew. Chem.* **2021**, *133*, 13769–13773.

[30] P. Erdmann, L. Greb, *ChemPhysChem* **2021**, *22*, 935–943.

[31] Details given in the Supporting Information.

[32] H. Großekappenberg, M. Reißmann, M. Schmidtmann, T. Müller, *Organometallics* **2015**, *34*, 4952–4958.

[33] a) F. Lips, J. C. Fettinger, A. Mansikkamäki, H. M. Tuononen, P. P. Power, *J. Am. Chem. Soc.* **2014**, *136*, 634–637; b) A. V. Protchenko, J. I. Bates, L. M. A. Saleh, M. P. Blake, A. D. Schwarz, E. L. Kolychev, A. L. Thompson, C. Jones, P. Mountford, S. Aldridge, *J. Am. Chem. Soc.* **2016**, *138*, 4555–4564; c) C. Shan, S. Yao, M. Driess, *Chem. Soc. Rev.* **2020**, *49*, 6733–6754.

[34] K. Inomata, T. Watanabe, Y. Miyazaki, H. Tobita, *J. Am. Chem. Soc.* **2015**, *137*, 11935–11937.

[35] J. V. Obligacion, P. J. Chirik, *Nat. Chem. Rev.* **2018**, *2*, 15–34.

[36] a) *Hydrosilylation: A Comprehensive Review on Recent Advances* (Ed.: M. Bogdan), Springer, Netherlands, **2009**; b) Y. Nakajima, S. Shimada, *RSC Adv.* **2015**, *5*, 20603–20616.